Mucosal-associated invariant T cells promote ductular reaction through amphiregulin in biliary atresia

Man-Huan Xiao,[a,b] Sihan Wu,[b] Peishi Liang,[b] Dong Ma,[b] Jiang Zhang,[c] Huadong Chen,[a] Zhihai Zhong,[a] Juncheng Liu,[a] Hong Jiang,[a,***] Xuyang Feng,[b,**] and Zhenhua Luo[a,b,*]

[a]Department of Pediatric Surgery, The First Affiliated Hospital, Sun Yat-sen University, Guangzhou, Guangdong, 510080, China
[b]Institute of Precision Medicine, The First Affiliated Hospital, Sun Yat-sen University, Guangzhou, Guangdong, 510080, China
[c]Department of Laboratory Medicine, The First Affiliated Hospital, Sun Yat-sen University, Guangzhou, Guangdong, 510080, China

eBioMedicine
2024;103: 105138
Published Online xxx
https://doi.org/10.1016/j.ebiom.2024.105138

Summary

Background Biliary atresia (BA) is a neonatal fibro-inflammatory cholangiopathy with ductular reaction as a key pathogenic feature predicting poor survival. Mucosal-associated invariant T (MAIT) cells are enriched in human liver and display multiple roles in liver diseases. We aimed to investigate the function of MAIT cells in BA.

Methods First, we analyzed correlations between liver MAIT cell and clinical parameters (survival, alanine transaminase, bilirubin, histological inflammation and fibrosis) in two public cohorts of patients with BA (US and China). Kaplan–Meier survival analysis and spearman correlation analysis were employed for survival data and other clinical parameters, respectively. Next, we obtained liver samples or peripheral blood from BA and control patients for bulk RNA sequencing, flow cytometry analysis, immunostaning and functional experiments of MAIT cells. Finally, we established two *in vitro* co-culture systems, one is the rhesus rotavirus (RRV) infected co-culture system to model immune dysfunction of human BA which was validated by single cell RNA sequencing and the other is a multicellular system composed of biliary organoids, LX-2 and MAIT cells to evaluate the role of MAIT cells on ductular reaction.

Findings Liver MAIT cells in BA were positively associated with low survival and ductular reaction. Moreover, liver MAIT cells were activated, exhibited a wound healing signature and highly expressed growth factor Amphiregulin (AREG) in a T cell receptor (TCR)-dependent manner. Antagonism of AREG abrogated the proliferative effect of BA MAIT cells on both cholangiocytes and biliary organoids. A RRV infected co-culture system, recapitulated immune dysfunction of human BA, disclosed that RRV-primed MAIT cells promoted cholangiocyte proliferation via AREG, and further induced inflammation and fibrosis in the multicellular system.

Interpretation MAIT cells exhibit a wound healing signature depending on TCR signaling and promote ductular reaction via AREG, which is associated with advanced fibrosis and predictive of low survival in BA.

Funding This work was funded by National Natural Science Foundation of China grant (82001589 and 92168108), National Key R&D Program of China (2023YFA1801600) and by Basic and Applied Basic Research Foundation of Guangdong (2020A1515110921).

Keywords: Biliary atresia; MAIT cells; Ductular reaction; AREG; TCR-dependent

Introduction

Biliary atresia (BA) is a devastating neonatal cholangiopathy featuring severe liver fibrosis and rapid progression to end stage liver disease.[1,2] BA is the leading indication for pediatric liver transplant worldwide.[3] In response to insults, such as viral infection, damaged cholangiocytes activate an innate and adaptive inflammatory response that eventually results in biliary obstruction.[4] Meanwhile, cholangiocytes initiate replication and proliferation, which together with other cells such as inflammatory cells is termed ductular reaction.[5,6] Ductular reaction is a maladaptive wound-healing

*Corresponding author. Number 1, Zhongshan Er Road, Yuexiu District, Guangzhou, Guangdong, 510080, China.
**Corresponding author. Number 1, Zhongshan Er Road, Yuexiu District, Guangzhou, Guangdong, 510080, China.
***Corresponding author. Number 1, Zhongshan Er Road, Yuexiu District, Guangzhou, Guangdong, 510080, China.
E-mail addresses: luozhh35@mail.sysu.edu.cn (Z. Luo), fengxy58@mail.sysu.edu.cn (X. Feng), jiangh38@mail.sysu.edu.cn (H. Jiang).

Research in context

Evidence before this study

Ductular reaction that is identified histologically as bile duct hyperplasia, is often observed in patients with cholestatic liver diseases including biliary atresia, and also identified in various liver diseases. Ductular reaction is often together with inflammatory cell infiltration in portal areas of livers, contributing to an abnormal wound-healing response and liver fibrosis. Thus, ductular reaction can be a therapeutic target to inhibit liver fibrosis. In biliary atresia, ductular reaction is associated with liver fibrosis and poor survival. However, the underlying mechanisms remain unknown.

Added value of this study

Our study show that mucosal-associated invariant T (MAIT) cells, which are abundant especially in the liver, were highly activated and exhibited a wound healing signature. Further, MAIT cells promoted ductular reaction via AREG, which clarify the regulation of rapid progression of fibrosis in biliary atresia.

Implications of all the available evidence

Our findings characterize the ductular reaction promoting potential of liver MAIT cells and suggest that MAIT cells could be a prognostic biomarker and potential therapeutic target for biliary atresia.

response which is associated with several liver disease progression[7–9] and has a key role in the initiation and progression of liver fibrosis.[10,11] In BA, higher presence of ductular reactions is an indication of extent of liver fibrosis and poor survival.[12,13] However, the mechanisms of ductular reaction remain poorly understood in BA.

Mucosal-associated invariant T (MAIT) cells are a unique innate-like T cell subset defined by co-expression of C-type lectin-like receptor CD161 and the invariant Vα7.2–Jα33 T cell receptor (TCR) in humans, which recognizes riboflavin metabolites[14,15] presented on the restriction molecule major histocompatibility complex (MHC)-related protein-1 (MR1).[16] MAIT cells are abundant especially in the liver compared to any other human tissues, with up to 15% in of total $CD3^+$ T cells.[17] In several liver diseases, MAIT cells are exposed to increased inflammatory cues and activated towards a cytotoxic or profibrogenic phenotype by a group of cytokines including IL-18 and IL-12.[18–21] This suggests a prominent role of MAIT cells both in liver inflammation and fibrogenesis. In addition, MAIT cells, activated by TCR stimulation, display a wound healing gene expression program.[22–24] It has been reported that MAIT cells express a wound healing program at steady state and have a wound healing function in the skin.[25,26] In mucosa, MAIT cells strengthened the colonic mucosal barrier by inducing the tight junction protein occludin.[27] Lung MAIT cells can also produce growth factors such as PDGF, VEGF and AREG, which play a role in repair.[22] AREG can promote epithelial cell proliferation, re-epithelialisation, and goblet cell activity, strengthening the mucus barrier.[28] Depending on the distinct tissue microenvironment, MAIT cells may express both antibacterial and wound healing functions at different stages in the evolution of an infectious or physical injury, and their role can be either pathogenic or protective. Further studies are required to understand the balance between their wound healing potential and their pro-inflammatory feature.

In this study, we investigate clinical implications and functions of MAIT cells using human liver transcriptomics data, freshly isolated liver MAIT cells from BA patients, rhesus rotavirus (RRV) infected human cholangiocytes and PBMC co-culture cell system, and human biliary organoids - LX-2 cells - MAIT cells multicellular system. We reported that liver MAIT cells were associated with histological inflammation and fibrosis, and predicted low survival in patients with BA. Liver MAIT cells were activated, located around portal tracts and positively correlated with bile duct profiles in BA. Using freshly isolated MAIT cells from BA patients, we found that BA MAIT cells exhibited a wound healing signature, and promoted human cholangiocyte proliferation and biliary organoids growth via AREG. Moreover, we developed a RRV infected co-culture cell system to recapitulate immune dysfunction of human BA and further validated the wound healing signature and ductular reaction-promoting functions of MAIT cells. RRV-primed MAIT cells promoted ductular reaction in the multicellular system. Finally, we found that this wound healing signature was dependent on MR1 mediated TCR signaling and AREG expression in BA liver was positively correlated with expression of MR1, ductular reaction markers, chemokines and RAS-MAPK signaling.

Methods

Detailed information of methods is provided in the Supporting materials. All antibodies used are listed in Supplemental Table S1. Primer sequences are listed in Supplemental Table S2.

Study design

The aim of this study was to identify the function of MAIT cells on BA. First, we analyzed correlations of liver MAIT cell level and clinical parameters [survival, alanine transaminase (ALT), bilirubin, histological inflammation and fibrosis] in two public cohorts of patients with BA (one cohort was 45 BA patients in US, while the second cohort was 102 BA patients in China). Next, we obtained liver or peripheral blood samples

from BA and control patients for bulk RNA sequencing (RNAseq), flow cytometry analysis, immunostaning, and performed wound healing experiment and cell proliferation assay in both chonlangiocyte cell line and biliary organoids. The control patients were pediatric patients with hepatoblastoma (HB), neonatal intrahepatic cholestasis (IHC) and congenital choledochal cysts (CC). For hepatoblastoma, we only obtained adjancent normal liver tissues for study. Finally, we established two *in vitro* co-culture systems, one is the RRV infected co-culture system to model immune dysfunction of human BA which was validated by single cell RNA sequencing (scRNA-seq) and the other is a multicellular system composed of biliary organoids, LX-2 and MAIT cells to evaluate the role of MAIT cells on ductular reaction.

Ethics statement

All human specimens were collected at The First Affiliated Hospital of Sun Yat-sen University, P.R. China. The protocol was approved by the Institutional Research Ethics Committee at The First Affiliated Hospital of Sun Yat-sen University (approval number 2021-572). The study design conformed to the ethical guidelines of the 1975 Declaration of Helsinki and Istanbul. Written informed consents were obtained from parents of each patient or patients.

The animal protocols were reviewed and approved by the Animal Care and Use Committee of Sun Yat-sen University (number SYSU-IACUC-2022-016).

Patients

Liver samples and peripheral blood were obtained from patients with BA and controls including hepatoblastoma, neonatal intrahepatic cholestasis and congenital choledochal cysts. These types of disease controls have been used in study of BA.[29–31] No matching was done between BA and controls. The diagnosis of BA was defined by an abnormal intraoperative cholangiogram and histological demonstration of obstruction of extrahepatic bile ducts. Liver samples of BA were obtained at the time of hepatoportoenterostomy (HPE). Adjacent normal liver tissues of human hepatoblastoma were collected at radical tumor resection. Clinical paramters including sex assigned at birth, age, ALT, aspartate transaminase (AST), gamma-glutamyl transferase (GGT), total bilirubin, liver pathology (histiological inflammation score and fibrosis score of liver section), failure of jaundice clearance, portal vein hypertension from patients with BA (n = 47) and controls (n = 41) were summarized in Supplemental Table S3. Age has been shown to be a potential confounding factor as it is associated with stage of disease and patient outcome.[4,32] Due to difficulty in obtaining perfect age matched control samples, our study enrolled BA and control patients with age in an appropriate range to minimize the confounding effect of age as previous studies.[31,33] Failure of jaundice clearance were determined by total bilirubin >34.2 μmol/L at 3 months after HPE as previous described.[34] Portal vein hypertension were defined by history of a complication including esophageal or gastric variceal bleed, ascites, or hepatopulmonary syndrome or clinical findings consistent with portal vein hypertension [both splenomegaly (spleen palpable >2 cm below the costal margin) and thrombocytopenia (platelet count <150,000/mL)] as previous described.[35] Every specimen from one patient was used for one or two different experiments.

Estimation of relative cell abundance of liver MAIT cells in two cohorts of patients with biliary atresia and association with clinical parameters

Level of liver MAIT cells was estimated in two cohorts of BA patients using single sample Gene Set Enrichment Analysis (ssGSEA) method with input of marker genes for MAIT cells and gene expression data as previously described.[36] The first cohort (the US cohort) was microarray gene expression data of 47 BA patients in USA, while the second cohort (the China cohort) was bulk liver RNAseq data of 102 patients with biliary atresia and 14 non-BA disease control patients.[37,38] Gene expression data were retrieved from previous deposition in the Gene Expression Omnibus database under accession number GSE15235 for the US cohort and in the Genome Sequence Archive of Beijing Institute of Genomics, Chinese Academy of Sciences under accession number HRA003331 for the China cohort. Clinical parameters including survival, ALT, bilirubin, histological inflammation and fibrosis of the US cohort and China cohort were retrieved from the original pubulications.[37,38] 2 patients in the US cohort were removed due to dropped off the study as described in the original publication.[30] Then, based on the median level of MAIT cells, patients were dichotomized into MAIT high- and low groups for two cohorts separately. For survival analysis, patients were followed started at the time of HPE surgery and ended at 24 months after HPE as described in the original publication.[37,38] None of these survival data are censored. Kaplan–Meier survival plots were generated and differences in survival were tested by Log-rank test. For other clinical parameters, spearman correlation was used to examine the correlation with level of MAIT cells and data were plotted using corrplot R package. The degree of correlation were defined by the following cutoff: absolute values of spearman correlation coefficient rho, 0–0.19 was regarded as very weak, 0.2–0.39 as weak, 0.40–0.59 as moderate, 0.6–0.79 as strong and 0.8–1 as very strong correlation.[39] The marker genes for MAIT cells were obtained from previous publications[40,41] and detailed listed at Supplemental Table S4.

Immunofluorescence staining (IF)

Immunofluorescence on frozen section was performed to examine localization of MAIT cells.

Liver mononuclear cell (LMNC) and PBMC isolation

LMNCs and PBMCs were isolated using density gradient centrifugation and cultured in RPMI medium (Corning, NY, USA) supplemented with 10% fetal bovine serum (FBS; FSP500, ExCell Bio, South America) and 1% Gibco Antibiotic-Antimycotic (15140122, Thermo Fisher Scientific, Waltham, MA, USA). Both cells were maintained in 37 °C incubators with 5% CO_2. LMNCs were isolated from liver tissues of control or BA patients. Liver tissue were dissociated in RPMI medium and filtered on a 70 μm cell strainer. LMNCs were isolated on a 33% Percoll density gradient.

In vitro stimulation assays

For detection of intracellular cytokines, LMNCs or PBMCs were stimulated for 4 h at 37 °C with phorbol 12-myristate 13-acetate (PMA; P1585, Sigma–Aldrich, St. Louis, MO, USA) and ionomycin (I0634, Sigma–Aldrich) at 10 ng/mL and 0.5 μg/mL, respectively, in the presence of brefeldin A (B7651, Sigma–Aldrich) at 3 μg/mL.

For IL-12 and IL-18 stimulation, cells were stimulated *in vitro* with 50 ng/mL IL-12 (200-12-10, PeproTech, CA, USA) and IL-18 (9124-IL-010, R&D Systems, Minneapolis, MN) for 24 h.

Flow cytometry

Human MAIT cells were identified as $CD3^+$ $CD161^+V\alpha7.2^+$ cells. Dead cells were excluded from the analysis using the Ghost Dye™ Red 710 (13-0871, Tonbo Biosciences, San Diego, CA, USA). Cells were labeled with cell surface antibodies before fixation and permeabilization using the Cytofix/Cytoperm slon kit (554,714, BD Biosciences, San Jose, CA, USA) as per the manufacturer's instructions. Cells were subsequently washed and stained for intracellular antibodies for flow cytometric analysis (LSR Fortessa X-20; BD Biosciences).

MAIT cells sorting

MAIT cells from BA or control patients were enriched as CD3 and Vα7.2 double positive cells from LMNCs or PBMCs by fluorescence-activated cell sorting on a LSR Fortessa X-20 (BD Biosciences). RRV-primed or uninfected MAIT were sorted as $CD3^+$ $V\alpha7.2^+$ $CD161^+$ cells.

RNAseq analysis of MAIT cells

MAIT cells were enriched from LMNCs from adjacent non-tumor liver tissues of HB patients (n = 4) or BA patients (n = 6). Total RNA were used as input material and libraries were prepared by following the SMARTer Stranded Total RNA-Seq kit-Pico Input Mammalian user manual in shanghai biotechnology. The RNA sequencing data has been deposited in GEO database (GSE217466) and can be accessed by token wrufaauodxczhit.

Wound-healing assay

Human cholangiocyte cell line H69 were cultured in 96-well plates. A total of 2×10^4 H69 cells were seeded per well in a 96-well clear flat bottom plate (Corning) and grown to confluency at 37 °C for 2 days and then scratched and washed with PBS before supplementing with different supernatants. Supernatants were collected at 5 days of sorted MAIT cells and diluted with RPMI medium containing 2% FBS in a ratio of 1: 3. Time lapse imaging was recorded every 4 h using microscopy (CKX53, Olympus, Tokyo, Japan) for 24 h. For anti-AREG blocking, 1 μg/mL of the polyclonal anti-AREG antibody was added to the supernatants. The open wound area were analyzed using ImageJ. The percentage of wound healing is defined as the quotient of the initial wound area and the wound area after a fixed time interval.

Cell counting assays

A total of 3×10^3 H69 cells per well were seeded in 96-well cell culture plates. Next day, 100 ng/mL cytokines were added to the cells or sorted MAIT cells were co-culture with the H69 cells. For anti-AREG blocking, 2 μg/mL of the polyclonal anti-AREG antibody was added. Cell viability was tested by Cell Counting Kit-8 (CCK8) assay (HY-K0301, MCE, New Jersey, United States) after 48 h.

In vitro co-culture experiments of human cholangiocytes and PBMCs

Human cholangiocyte H69 were grown to 80% confluency before infection. RRVs were treated with trypsin at a concentration of 4 μg/mL in DMEM (Corning) for 1 h. Cells were washed with PBS for three times and infected with pretreated RRVs at an MOI of 1 for 1 h. Cells were then washed with PBS and co-cultured with freshly isolated PBMCs derived from healthy donors at the ratio of 1:2 (H69: PBMC). After co-culturing for 48 h, living $CD45^+$ cells were sorted using Ghost Dye™ Red 710 and PE/Cyanine7-conjugated anti-CD45 antibody.

For intracellular staining, PBMCs co-culturing for 18 h were stimulated with PMA/ionomycin/brefeldin A for 4 h and the intracellular cytokine expression was analyzed by flow cytometry. For anti-MR1 blocking, 2 μg/mL of the monoclonal anti-MR1 antibody was added during co-culturing.

Single cell RNA sequencing (scRNA-seq) and data analysis

Single cell RNA sequencing libraries were performed according to the manufacturer's instructions (single cell 3′ v2 protocol, 10× Genomics). The libraries were sequenced in Illumina NovaSeq 6000. The demultiplexing, barcoded processing, gene counting and aggregation of sequencing data were made using the Cell Ranger software v2.1.1. The scRNA-seq data has been deposited in GEO database (GSE225177) and can be accessed by token utyngeyohhqpjsb. Sequencing data were processed with Seurat (v3) single-cell analysis pipeline with modifications. All

subsequent scRNA-seq analyses were conducted using the Seurat R package (v3.2.2). Detailed information of scRNA-seq analyses is provided in the Supporting materials.

Pairwise overlapping comparisons of differentially expressed genes between RRV infected cell system and human BA liver

Differentially expressed genes for the RRV infected cell system were identified between RRV infected and uninfected groups. Differentially expressed genes for human BA livers were identified between 121 BA livers and 7 normal livers from our previous publication.[33] Pairwise overlapping comparisons were examined by Fisher's exact test in R.

Estimation of cell abundance of immune cell types in 121 patients with biliary atresia and 7 normal controls

Level of immune cell types identified in the RRV infected cell system were measured in 121 patients with BA and 7 normal controls using ssGSEA method with top 20 upregulated genes for each immune cell type and liver expression data as input as previously described.[36] Differnece of each immune cell type between BA and NC were tested by wilcoxon rank sum test. Liver expression data of 121 patients with BA and 7 normal controls was obtained from our previous publication.[33] Top 20 upregulated genes for each immune cell type were identified from scRNA-seq of the RRV infected cell system and listed in Supplemental Table S5.

MAIT cells and biliary organoid co-culture

Human biliary organoids were derived from adjacent normal tissues of hepatoblastoma from two patients and cultured as previous described.[42] For co-culturing, biliary organoids were trypsinized to single cells for 10 min, After dissociation, 3×10^3 cells was resuspended in growth factor reduced Matrigel (356,231, Corning). Droplets (25 μL) were plated per well into a 24-well plate and allowed to solidify for 10 min at 37 °C before adding 500 μL expansion medium, in which the concentration of recombinant human epidermal growth factor (hEGF; AF-100-15, PeproTech) was adjusted to 2.5 ng/mL. Sorted MAIT cells were added to the media for co-culture. For anti-AREG blocking, 2 μg/mL of the polyclonal anti-AREG antibody was added to the media and supplied every 2 days.

Generation of biliary organoid–LX-2 multicellular system

Biliary organoids were trypsinized to single cells and mixed with LX-2 cells at the ratio of 1:2 (organoid: LX-2). 3×10^3 mixed cells was resuspended in Matrigel (25 μL) and plated into a 48-well plate for 7 days in expansion medium without TGF-β inhibitor A83-01 and Rho kinase inhibitor Y-27632 dihydrochloride, and then co-cultured with sorted MAIT cells for 3 days.

Analysis of gene expression

The levels of RNA were detected by real-time quantitative RT-PCR (qPCR).

Statistics

Correlations among liver MAIT cells, clinical parameters were performed using spearman correlation and plotted with corrplot R package. For statistical analysis, every patient represented once in any statistical test.

Data are expressed as the mean ± standard deviation (SD) of the indicated number of samples and are from at least three independent experiments or one experiment representative of at least three performed. Differences between two groups were analyzed using either Student's t-test when the variances are equal (normally distributed) or Mann–Whitney test when they are not. All statistical tests were two sided. Differences were considered statistically significant at $p < 0.05$. Analyses were performed using the GraphPad Prism program V.6 (GraphPad, San Diego, CA).

Role of funders

The funders were not involved in study design, data collection, analysis, interpretation, or writing.

Results

Liver MAIT cells are associated with low survival, advanced fibrosis and ductular profiles in BA

To investigate the clinical implications of liver MAIT cells in human BA, we first performed survival analysis of liver MAIT cells with transplant-free survival after HPE in two cohorts of BA patients. The first cohort (the US cohort) was microarray gene expression data of 47 BA patients in USA, while the second cohort (the China cohort) was bulk liver RNAseq data of 102 BA and 14 non-BA disease control patients[37,38] at the time of diagnosis. 2 patients in the US cohort were removed due to dropped off the study as described in the original publication.[30] The abundance of liver MAIT cells were estimated with ssGSEA using marker genes for MAIT cells (Supplemental Table S4). ssGSEA is a gene rank-based method that calculates an enrichment score for each sample and indicates the abundance of MAIT cells. When dichotomizing the patients into MAIT high- and low groups based on median level of liver MAIT cells, we found that patients with high level of liver MAIT cells (MAIT high group) displayed lower survival in both cohorts (Log-rank $P = 0.0108$ in the US cohort and $P = 0.0144$ in the China cohort, Fig. 1A and B).

Liver injury, ductular reaction and liver fibrosis has been reported to predictive of low survival in BA.[12,33,43] Thus, we performed correlation analysis among levels of liver MAIT cells, clinical parameters at diagnosis [Serum ALT and conjugated bilirubin (CB) or total bilirubin (TB)], liver pathology (histological inflammation and fibrosis), and expression of *KRT19* (a marker

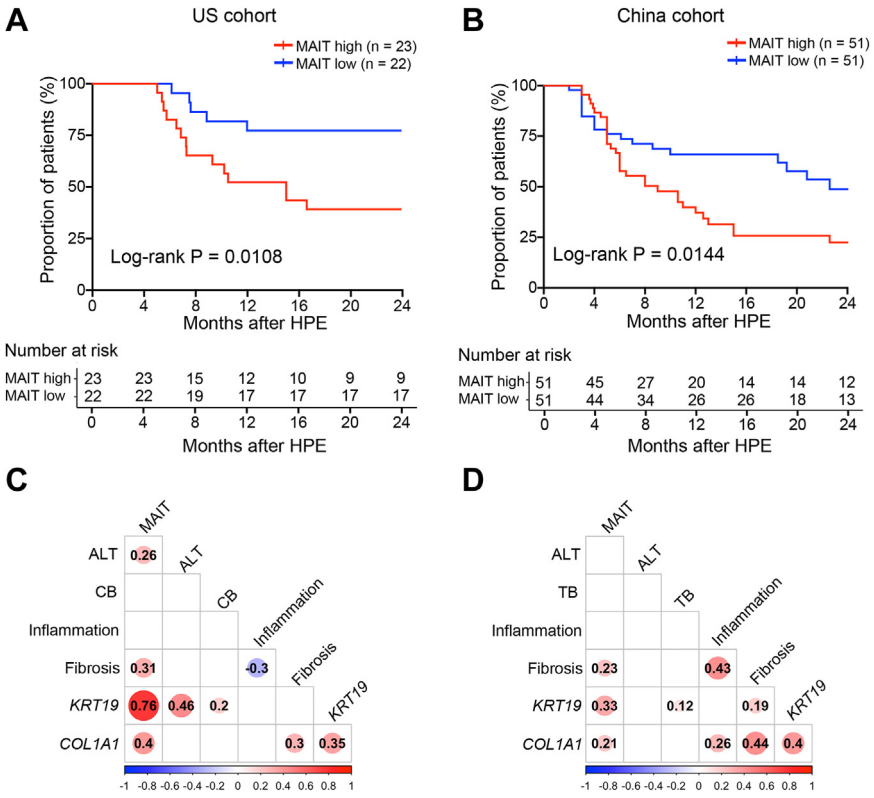

***Fig. 1:* Liver MAIT cells predict low survival and are associated with liver cirrhosis signatures**. (**A and B**) Kaplan–Meier plots of survival of biliary atresia patients with native liver after hepatoportoenterostomy (HPE) in (A) US cohort and (B) China cohort. *p* value was calculated by Log-rank test. The patients were stratified into the high- and low MAIT groups based on the median level of liver MAIT cells. (**C and D**) Spearman correlation matrix among liver MAIT cells, serum parameters at diagnosis (ALT and CB, conjugated bilirubin or TB, total bilirubin), histological inflammation and fibrosis, expression of *KRT19* and *COL1A1* in US cohort (C) and China cohort (D). Spearman correlation coefficients are shown only in boxes with spearman correlation *p* value < 0.05. Red indicates positive correlation, while blue indicates negative correlation. Dot size is proportional to absolute value of correlation coefficient.

for cholangiocytes), *COL1A1* (a marker for fibroblasts). Among these parameters, liver MAIT cells were positively correlated with histological fibrosis (rho = 0.31, $p = 0.035$ in US cohort; rho = 0.23, $p = 0.006$ in China cohort), expression of *KRT19* (rho = 0.76, $p < 0.0001$ in US cohort, rho = 0.33, $p = 0.005$ in China cohort) and *COL1A1* (rho = 0.4, $p = 0.011$ in US cohort, rho = 0.21, $p = 0.007$ in China cohort) in both cohorts (Fig. 1C and D). These human data suggest molecular links among liver MAIT cells, ductular reaction and liver fibrosis.

Liver MAIT cells exhibit activation phenotype and reside around portal tracts in patients with BA

To understand function of MAIT cells in BA, we obtained liver samples and peripheral blood were obtained from patients with BA and controls. Clinical information of these patients were summarized in Supplemental Table S3. To investigate how liver MAIT cells regulate ductular reaction, we first examined the abundance of liver MAIT cells in clinical samples. Using flow cytometry analysis, we found that the frequency of MAIT cells ($CD3^+CD161^+V\alpha7.2^+$) among $CD3^+$ T cells were significantly reduced in both liver and peripheral blood in BA when compared with the control (Fig. 2A). The frequency of MAIT cells were confirmed by using MR1-5-OP-RU Tetramer staining, which was comparable with staining with Vα7.2 (Supplemental Fig. S1). We thus used Vα7.2 staining for identifying MAIT cells hereafter. MAIT cells from BA exhibited higher activation (marked by HLA-DR and CD38) (Fig. 2B). This is consistent with previous studies showing that liver MAIT cells decreased but were activated in liver diseases.[21,44]

The localization of liver MAIT cells was visualized by immunofluorescence staining for CD3 and TCR Va7.2 in human liver samples from BA and adjacent normal liver tissues of hepatoblastoma as control. Most MAIT cells (marked by $CD3^+$ TCR $V\alpha7.2^+$) localized around portal tracts in both BA and control (Fig. 2C and Supplemental Fig. S2). Examining the correlation among the abundance of liver MAIT cells measured by flow cytometry, level of clinical parameters and

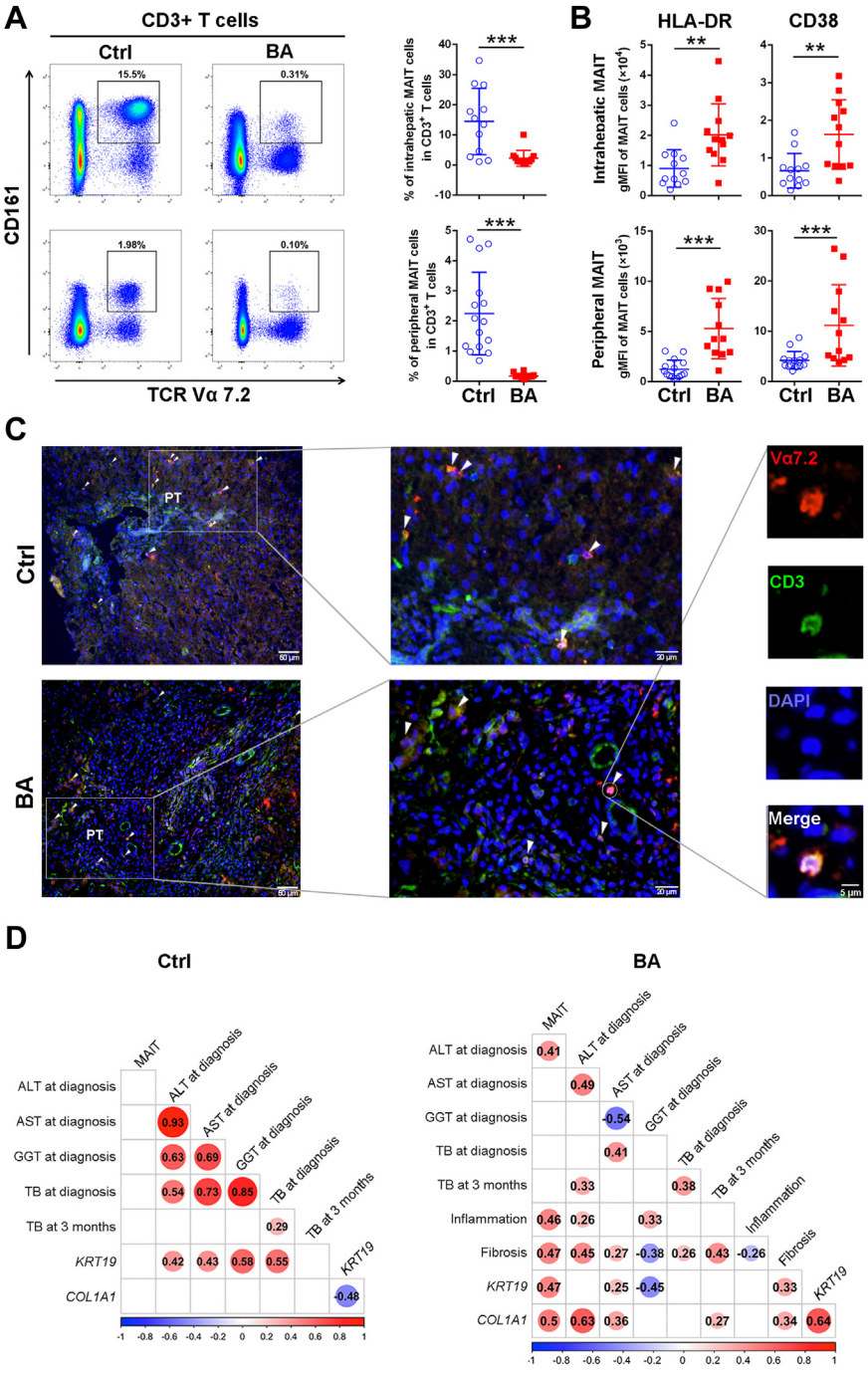

Fig. 2: **MAIT cells display low frequency but high activation and reside around portal tracts in BA liver tissues**. (**A**) Representative dot plots and percentages of intrahepatic and peripheral MAIT cells among CD3$^+$ T cells in the control (n = 12, 15) and BA (n = 12, 12) livers or peripheral bloods, respectively. (**B**) Comparison of expression of HLA-DR and CD38 on intrahepatic and peripheral MAIT cells in control (n = 12) and BA (n = 12) patients. (**A-B**) Statistical analysis was performed using Student's t test or Mann–Whitney test depending up on the distribution turns in to the normal or not. Data points are mean ± SD. $^{**}p < 0.01$, $^{***}p < 0.001$. (**C**) Representative images of CD3$^+$ (green) Vα7.2$^+$ (red) double positive cells (white arrowheads) in liver tissue sections from control (n = 3) and BA (n = 3) liver tissues. Colocalization of CD3 and Vα7.2 (see higher magnification at right panels) identifies MAIT cells. White box in left panels point at a portal field (middle panels). PT, portal tract. Nuclei were stained with DAPI (blue). (**D**) Correlation matrix among abundance of MAIT cells measured by flow cytemetry, level of clinical paramters, expression *KRT19*, *COL1A1*. Spearman correlation coefficients are shown only in boxes with spearman correlation *p* value < 0.05. Red indicates positive correlation, while blue indicates negative correlation. Dot size is proportional to absolute value of correlation coefficient.

expression of cholangiocyte marker *KRT19*, fibrosis marker *COL1A1* in the same patients (n = 12 for BA, n = 12 for control), we observed that liver MAIT cells were positively correlated with histological inflammation (Spearman correlation rho = 0.46 and $p = 0.0485$) and fibrosis (rho = 0.47 and $p = 0.0102$) (Fig. 2D and Supplemental Table S6). Moreover, liver MAIT cells were correlated with expression of *KRT19* and *COL1A1* only in BA patients (rho = 0.47 and $p = 0.0210$ for *KRT19*, rho = 0.50 and $p = 0.0296$ for *COL1A1*) but not in control (Fig. 2D and Supplemental Table S6).

Activated MAIT cells highly express AREG and promote cholangiocyte proliferation and migration

To understand molecular characteristic of MAIT cells, we sorted MAIT cells from liver samples of BA and from adjacent normal liver tissue of hepatoblastoma (as control) for bulk RNAseq analysis. We identified 1199 upregulated and 728 downregulated genes in liver MAIT cells from BA (Fig. 3A). Differential expression analysis revealed that several growth factors (such as AREG) were upregulated in BA MAIT cells (Fig. 3A). Among these growth factors, AREG showed the largest upregulation (14.8 fold upregulated, $p = 0.0000157$) in BA MAIT cells (Supplemental Table S7). Functional enrichment analysis showed that top 10 upregulated biological processes (such as response to wounding, tube morphogenesis, epithelium development) were associated with ductular reaction, while neural related biological processes were downregulated in BA compared to control (Fig. 3B and C). These data was in line with our clinical observations in two BA cohorts that MAIT cells might promote maladaptive wound healing response in BA.

To determine MAIT function on cholangiocyte, we performed wound-healing assay by treating the human cholangiocyte cell line H69 with culture supernatants of MAIT cells derived from BA or control. Supernatants obtained from BA MAIT cell cultures significantly accelerated wound closure (Fig. 3D). Similary, the proliferation-promoting effect of MAIT cells on human cholangiocyte H69 was also validated by CCK8 assay (Fig. 3E). These data suggest that MAIT cells from BA promote cholangiocyte proliferation and migration.

To examine by which growth factor MAIT cells promote cholangiocyte proliferation, we first performed CCK8 assay of cholangiocyte cell line H69 under treatment of AREG, HB-EGF, IGF2 or VEGFA (candidates from Fig. 3A). We found that AREG and HB-EGF had the strongest and similar effect on promoting proliferation of cholangiocyte cell line H69 (Supplemental Fig. S3). As AREG displayed the highest upregulation among these growth factors in sorted BA MAIT cells (from Fig. 3A and Supplemental Table S7), we focused on AREG in the following experiments. To validate AREG expression in protein level, we detected the production of AREG and other effector cytokines in MAIT cells via flow cytometry. Consistent with the result of RNAseq, liver MAIT cells in BA highly expressed growth factor AREG as well as peripheral BA MAIT cells, while other pro-inflammatory or cytotoxic factors remains unchanged (Fig. 3F). Testing the effect of MAIT cells derived AREG on cholangiocytes, we found that accelerated wound closure induced by MAIT cells were blocked by AREG antibody (Fig. 3G). These results together provide initial evidence that MAIT cells in BA exhibited a wound healing signature and promoted cholangiocyte proliferation via AREG.

A RRV infected cell system recapitulates immune dysfunction of human BA

As human liver samples of BA were limited, using clinical liver samples for functional and cellular study was challenged sometimes. Moreover, we observed that MAIT cells in neonatal mice were undetectable in naive or RRV-induced mice (Supplemental Fig. S4), hampering the study of MAIT cells using disease mouse model of BA. To further study human MAIT cells in BA, we developed a new cell system by co-culture of RRV infected human cholangiocyte H69 with human PBMC from healthy donors (Fig. 4A). In this system, human cholangiocyte cell line H69 were infected by RRV, an important cause of BA.[45,46] The RRV infected or uninfected (as control) cholangiocytes were co-cultured with human healthy PBMC to mimic the immune environment in human BA (Fig. 4A). To characterize this cell system, we sorted CD45 positive cells from both groups for single cell RNA sequencing (Fig. 4A). The scRNA-seq analysis identified 10,214 and 10,028 cells in uninfected and RRV infected groups, respectively. This analysis revealed major immune cell types including naïve T cells ($CD3D^+CCR7^+SELL^+$), memory T cells ($CD3D^+S100A4^+$), MAIT cells ($CD3D^+SLC4A10^+$), cytotoxic T cells ($CD3D^+GZMB^+PRF1^+$), CD56 dim NK cells ($NCAM1^+KLRF1^+$), CD56 bright NK cells ($NCAM1^{++}KLRF1^+$), naïve B cells ($MS4A1^+IGHD^+IGHG1^-$), memory B cells ($MS4A1^+IGHD^-IGHG1^+$), monocytes ($CD14^+LYZ^+$) and dendritic cells ($CD14^-LYZ^+$) (Fig. 4B and C and Supplemental Table S8). Comparing these immune cells between RRV infected and uninfected groups, we found that MAIT cells were decreased while cytotoxic T cells, naïve B cell were increased in RRV infected group compared to uninfected group (Fig. 4D and Supplemental Table S8). These data was in line with several previous observations that innate and adaptive immune cells were increased and infiltrated in BA livers.[47,48]

In addition, differential expression and gene set enrichment analysis (GSEA) between RRV infected and uninfected groups showed that enrichment of immune related hallmarks gene sets including HALLMARK_INFLAMMATORY_RESPONSE (NES = 1.25, FDR = 0.019) and HALLMARK_INTERFERON_GAMMA_RESPONSE (NES = 1.29, FDR = 0.011) in the RRV infected

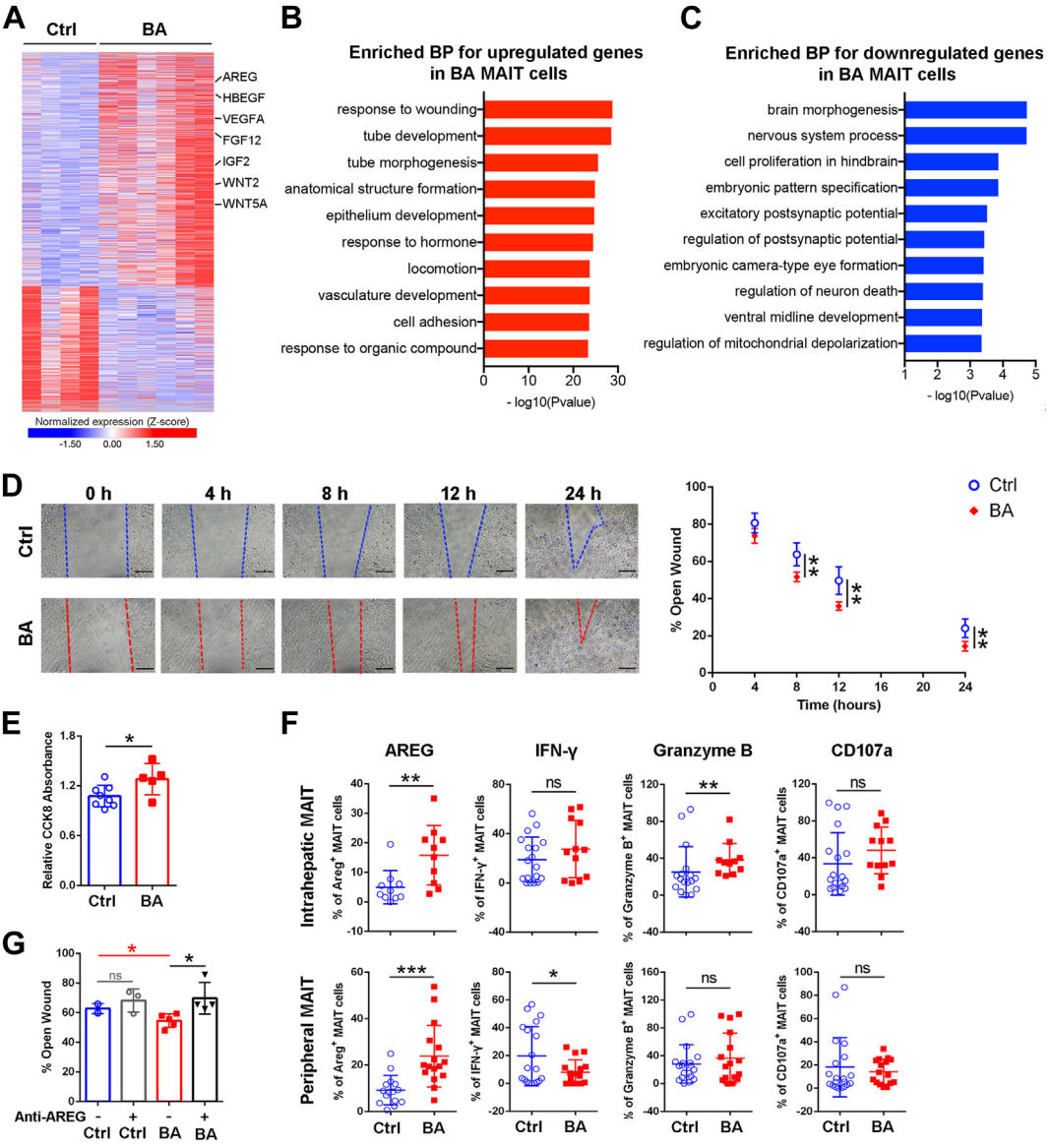

***Fig. 3*: Activated BA MAIT cells display a wound healing signature and promote cholangiocyte proliferation**. (**A**) Heatmap showing the expression of differentially expressed genes between BA (n = 6) and control (n = 4). Red indicates high expression, while blue indicates low expression. Upregulated genes related to wound healing signature are labelled. (**B and C**) Top 10 enriched biological processes for upregulated (B) or downregulated (C) genes in BA compared to control. (**D**) Representative images and summary data of the closure of the wounds in human cholangiocyte H69 were assessed with time-lapse imaging over a time course of 24 h. Cells were supplemented with different supernatants collected from 5-day co-cultures of sorted MAIT cells from control or BA peripheral bloods. The open wound areas were quantified as percentages of the initial wound size. Scale bars, 200 μm. (**E**) Cell viability was analyzed by CCK8 assay. Cells were co-cultured with sorted MAIT cells from control (n = 8) or BA (n = 5) peripheral bloods for 48 h. (**F**) Comparison of cytokine profile of BA (n = 10–16) vs. control (n = 10–19) intrahepatic and peripheral MAIT cells. Statistical analysis was performed using Student's t test or Mann–Whitney test depending on the distribution turns in to the normal or not. (**G**) The open wound areas of H69 supplemented with sorted MAIT cell cultures [BA (n = 5) vs. control (n = 4)] in the presence or absence of anti-AREG antibodies (1 μg/mL) were assessed at 8 h. Statistical analysis was performed using Student's t test. Data points are mean ± SD or mean, respectively. *$p < 0.05$, **$p < 0.01$, ***$p < 0.001$. ns, not significant.

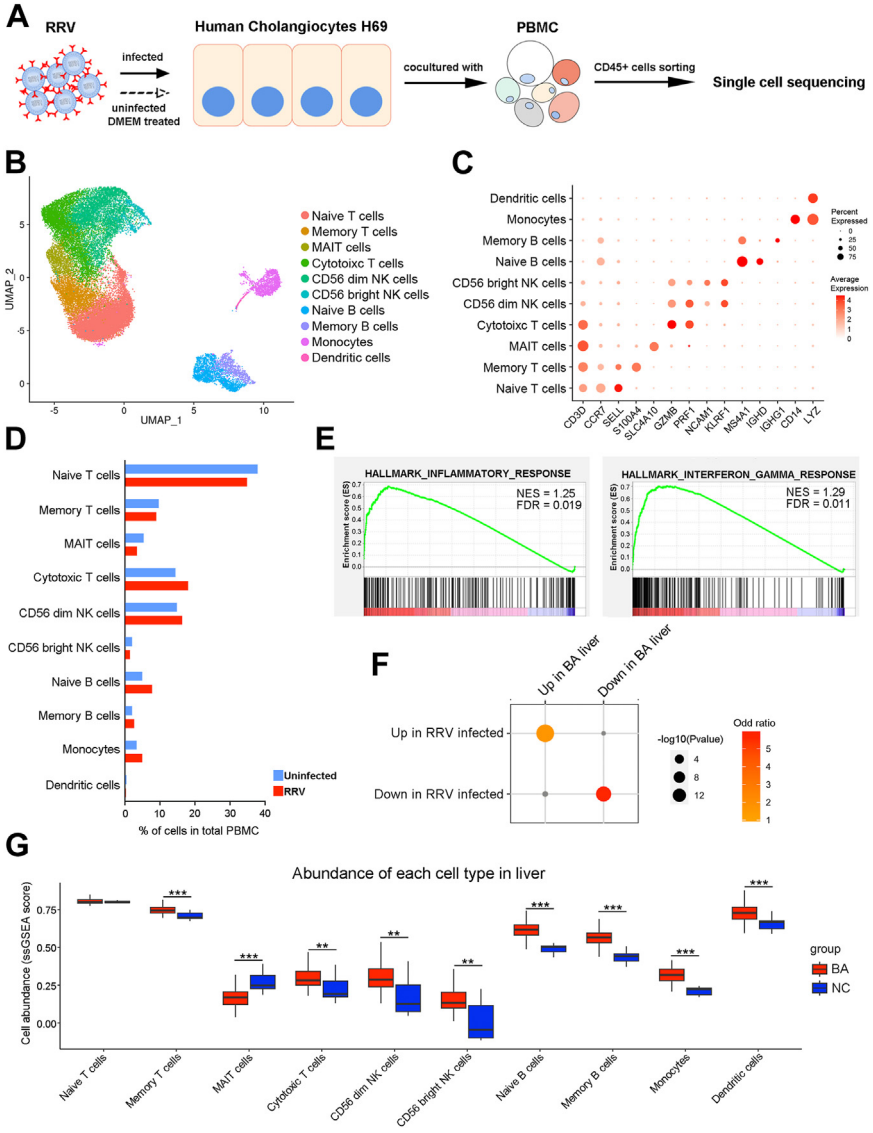

***Fig. 4:* A RRV infected cell system mimics immune environment of human BA liver**. (**A**) Diagram of the co-culture system. H69 were infected with RRVs at an MOI of 1 for 1 h, washed and co-cultured with human healthy PBMCs for 48 h. $CD45^+$ cells were sorted by flow cytometry for single cell RNA sequencing. (**B**) UMAP plot showing clusters of immune cell types. (**C**) Dotplot showing expression of key markers for each immune cell type. Size of dot is proportional to percentage of cell expressing the key marker. Red indicates the average of expression of the key marker. (**D**) Barplot showing percentage of each immune cell type in total PBMC in uninfected (blue) and RRV infected (red) groups. (**E**) GSEA plot showing enrichment of gene sets in RRV infected group compared to uninfected group. (**F**) Pairwise overlapping comparisons were performed between upregulated or downregulated genes in RRV infected group compared to uninfected group (Y axis) and upregulated or downregulated genes in human BA liver compared to normal liver (X axis) were examined by Fisher's exact test and shown as dots whose size is proportional to $-\log_{10}$ (p value) and gradation of red is proportional to odd ratio. (**G**) Abundance of each immune cell type in liver of BA and normal controls (NC) measured by ssGSEA method with Top 20 upregulated genes for each immune cell type and liver expression data of 121 BA patients and 7 normal controls (NC) as input. Differnece of each immune cell type between BA and NC were tested by wilcoxon rank sum test. $^{**}p < 0.01$, $^{***}p < 0.001$.

group (Fig. 4E). These data suggest that the RRV infected cell system display immune features akin to RRV infected mice model and human BA patients.[49,50] To evaluate clinical implication of this RRV infected cell system, we performed gene overlapping analysis of differentially expressed genes between the RRV infected cell system and human BA livers. Differentially expressed genes for human BA livers were identified between 121 BA livers and 7 normal livers from previous publication.[33] This gene overlapping analysis revealed a transcriptomic similarity between the RRV

infected cell system and human BA livers (Fig. 4F). To assess cell similarity, we estimated immune cell types in these 121 BA livers and 7 normal livers with ssGSEA method using top 20 upregulated genes (as gene signature) for each immune type identified in scRNA-seq data of the RRV infected cell system. In line with several previous studies, BA livers contain high levels of cytotoxic T cells, NK cells, B cells, monocytes and dendritic cells (Fig. 4G).[47,51,52] Consisent with flow cytometry data in Fig. 2A, BA livers showed less abundance of MAIT cells compared to control (Fig. 4G). All these data together indicate that the RRV infected cell system exhibit immune dysfunction similar to those in human BA liver.

RRV-primed MAIT cells display wound healing signature and promote cholangiocyte proliferation and migration via AREG

Having established a RRV infected cell system for human BA, we next sought to investigate the function of MAIT cells in this cell system. GSEA analysis revealed that RRV-primed MAIT cells (from RRV infected group) displayed enrichment of wound healing signatures (gene set: GOBP_WOUND_HEALING, GOBP_RESPONSE_TO_WOUNDING, GO_INFLAMMATORY_RESPONSE_TO_WOUNDING), suggesting MAIT cells in this cell system also display wound healing signature as liver MAIT cells from clinical samples (Fig. 5A). Examing wound healing related upregulated genes (from upregulated genes in Fig. 3B) in scRNA-seq data of RRV infected cell system, we found that AREG had the highest expression level among them and that RRV primed MAIT cells exhibited higher expression of AREG when compared to uninfected MAIT cells (Fig. 5B). These data was in keep with the findings of bulk RNAseq data of BA MAIT cells (see Fig. 3A and Supplemental Table S7). Therefore, we employed this cell system for functional studies (Fig. 5C). Flow cytometry analysis showed a decreased frequency of MAIT cells (Fig. 5D), activation of MAIT cells (Fig. 5E) and increased expression of AREG in MAIT cells (Fig. 5F) in the RRV infected group, which was similar with the observation in liver MAIT cells from clinical samples (see Fig. 2A and B and Fig. 3F). Wound-healing assay revealed that supernatants from RRV-primed MAIT cells culture promoted cholangiocyte wound closure, while antagonism of AREG abrogated the effect (Fig. 5G and H). Cell proliferation CCK8 assay also showed that RRV-primed MAIT cells promoted cell growth of H69 via AREG (Fig. 5I).

MAIT cells promote biliary organoid growth via AREG

Biliary organoids are self-organizing three-dimensional structures derived from bile ducts and suitable for the study of bile duct and disease modelling.[53] Thus, we co-cultured human biliary organoids derived from normal liver tissues with MAIT cells to further explore its function in promoting ductular reaction. The viability and functionality of biliary organoids were confirmed by a 7-days time-lapse imaging (Supplemental Fig. S5A) and Rhodamine123 assay (Supplemental Fig. S5B) as previously described.[54] As expected, biliary organoids co-cultured with MAIT cells from human BA liver significantly increased their diameters as compared to control (Fig. 6A). Similarly, diameters of biliary organoids significantly increased when co-cultured with RRV-primed MAIT cells from our RRV infected cell system (Fig. 6B). This effect was abrogated by blocking AREG (Fig. 6B). These results confirmed that MAIT cells promoted biliary organoid growth via AREG.

MAIT cells promote ductular reaction in biliary organoid–LX-2–MAIT cells multicellular system

In addition to cholangiocyte proliferation, inflammation and fibrosis are key features of ductular reaction. We noticed that MAIT cells were positively correlated with liver fibrosis (see Fig. 1C and D). To further explore the effect of MAIT cells in inducing inflammation and fibrosis, we evaluated MAIT cell function in a human biliary organoid–hepatic stellate cells LX-2–MAIT cells multicellular system (Fig. 6C). RRV-primed MAIT cells upregulated the expression of inflammatory genes *CCL2, IFNG* and profibrogeneic factor *TGFB1* (Fig. 6D) in the human biliary organoids–LX-2 multicellular system. Moreover, hepatic stellate cells activation marker *TIMP1* were induced by RRV-primed MAIT (Fig. 6E). These data suggested that inflammation and hepatic stellate cells activation were induced by RRV-primed MAIT cells following cholangiocyte proliferation. Interestingly, no difference was found in the activation of LX-2 when it was treated with supernatants from BA patients (Supplemental Fig. S6A) or co-cultured with RRV-primed MAIT cells (Supplemental Fig. S6B). These data together implicate that MAIT cells directly act on cholangiocyte followed by activation of inflammation and fibrosis, leading to ductular reaction eventually.

AREG expression in MAIT cells is TCR-dependent

MAIT cells can be activated by cytokines (such as IL-12 and IL-18) or TCR-dependent pathways.[17] To investigate regulation of AREG expression in MAIT cells, we first treated MAIT cells isolated from clinical samples of BA or control with exogenous IL-12 and IL-18. AREG expression remains unchanged after IL-12 and IL-18 stimulation in both control and BA groups whereas IFN-γ and Granzyme B were increased (Fig. 7A). Next, to test if AREG expression was dependent upon MR1-antigen-TCR interaction, we blocked the TCR mediated activation with a monoclonal anti-MR1 antibody in RRV infected cell system. The AREG production of RRV-primed MAIT cells was significantly reduced upon TCR blockade, while there was no difference in IFN-γ and Granzyme B (Fig. 7B). Taken all together, these data indicate that AREG production is dependent on TCR stimulation.

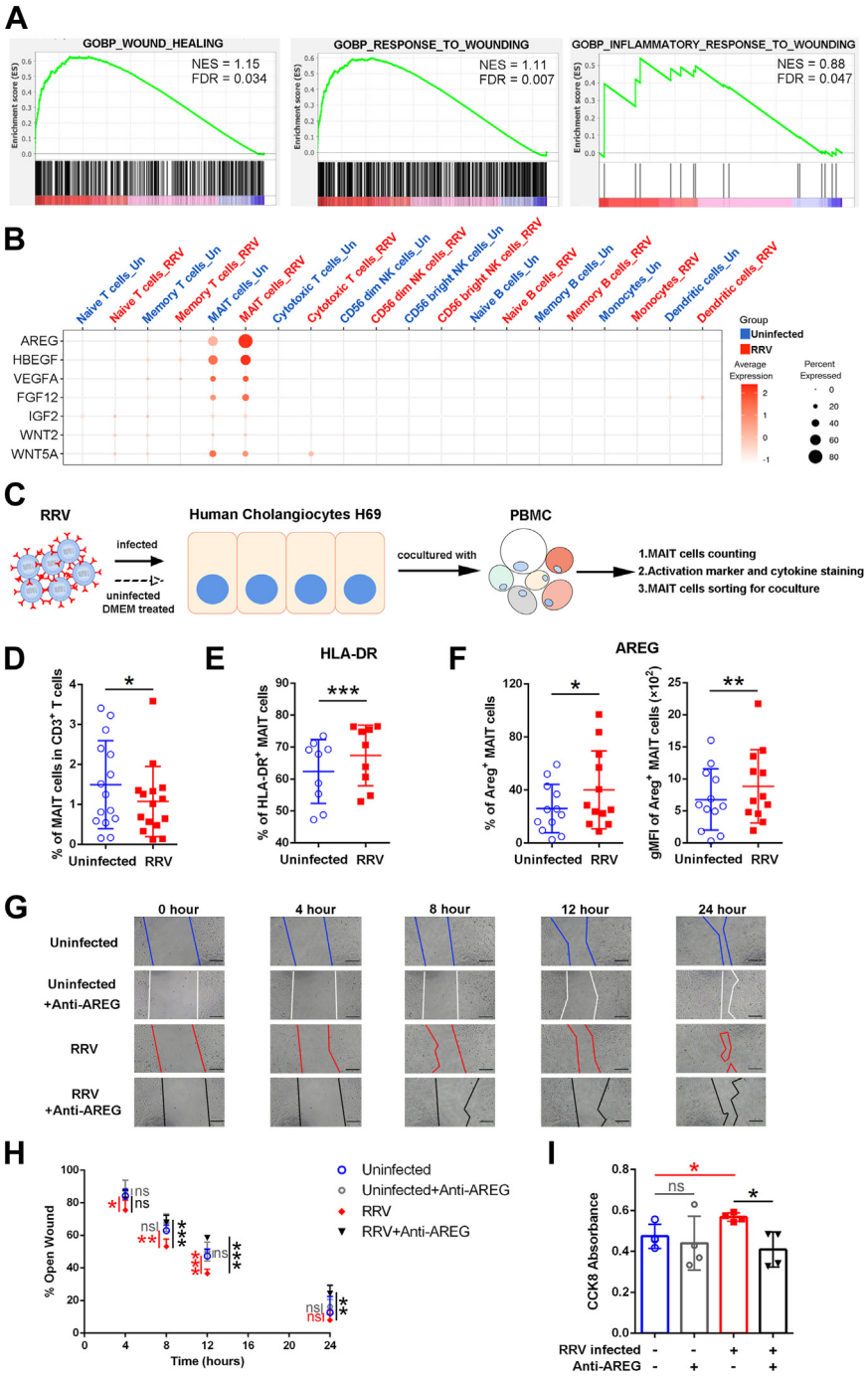

Fig. 5: **MAIT cells are activated and promote cholangiocyte proliferation after co-cultured with RRV-infected human cholangiocytes**. (**A**) GSEA plot showing enrichment of wound healing related gene sets in RRV-primed MAIT cells compared to those in uninfected group. (**B**) Dotplot showing expression of wound healing related upregulated genes identified in Fig. 3A for each immune cell type in scRNA-seq data of RRV infected cell system. In X axis, blue denotes immune cell types from uninfected group, while red denotes immune cell types from RRV infected group. Size of dot is proportional to percentage of cell expressing the key marker. Red indicates the average of expression. (**C**) Diagram of the co-culture system. (**D–F**) Analysis of frequency (D), activation marker (E) and intracellular cytokine production (F) of MAIT cells from RRV-primed vs. uninfected group (n = 9–15). PBMCs co-cultured with RRV-infected human cholangiocytes H69 for 18 h, followed by activation marker and intracellular cytokine staining. (**G and H**) Representative images (G) and summary data (H) of the closure of the wounds in human cholangiocytes H69 were assessed with time-lapse imaging over a time course of 24 h in the presence or absence of anti-AREG antibody.

Liver AREG expression is positively correlated with expression of MR1, ductular reaction markers, chemokines and RAS-MAPK

To further understand potential upstream and downstream factors of AREG, we performed correlation analysis between AREG and some key factors related to BA pathogenesis[4,50] in liver gene expression of two BA cohorts (the US and China cohorts we used in Fig. 1). Confirming the observations that AREG production was dependent on TCR stimulation and that AREG promoted ductular reaction, liver AREG were positively correlated with MR1, ductular reaction marker (*KRT19*, *COL1A1*) (Fig. 7C). Interestingly, AREG had strong correlation with CCL2, CXCL2, CXCL8, suggesting that MAIT cells might have interaction with other immune cells such as macrophages and neutrophils. Regarding the downstream effectors, AREG were linked to RAS-MAPK signaling (KRAS, MAPK1, MAP2K1).

Discussion

In mice, MAIT cells are about 100-fold less abundant than in human[55] and there was a dearth of MAIT cells in the skin, lungs, and intestines of 2-week old mice.[25] Consistently, we found that liver MAIT cells are barely detected in neonatal normal and RRV infected BALB/c mice within 2 weeks after birth. As the difference in MAIT cells between human and mouse, the classical experimental mouse model for BA can not fully mimic immune microenvironment of human BA and is not suitable for studying MAIT cell function. Directly studying clinical specimens from BA patients or developing a new human-based model is necessary for understanding pathogenic mechanisms of human BA. In this study, the freshly isolated MAIT cells from BA clinical specimens were used to explore their functional roles, which reflected the primordial state of MAIT cells in human BA. In addition, we established a new RRV infected co-culture cell system to mimic immune dysfunction of human BA and found a transcriptomic and cell similarity between our RRV infected cell system and human BA livers. MAIT cells from this RRV infected co-culture cell system exhibit similar functionality of wound healing with those from human BA livers, demonstrating clinical relevance of this cell system. Accordingly, this *in vitro* co-culture system can also be exploited for exploring other immune cell functions in BA.

In liver, MAIT cells can secrete pro-inflammatory, cytotoxic and fibrogenic molecules, including IFN-γ, Granzyme B, TNF-α, and IL-17.[56] Combined with their abundance in the liver, MAIT cells play a prominent role both in liver inflammation and fibrogenesis. In autoimmune liver disease, MAIT cells participate in liver fibrosis via enhancing hepatic stellate cell activation.[57] In viral hepatitis, however, MAIT cells exhibited a flawed phenotype and impairment of immune response function.[58–60] In cholangiopathy such as primary biliary cholangitis, IL-7 promotes the production of inflammatory cytokines and Granzyme B in MAIT cells.[61] Therefore, MAIT cells play complex roles in a context dependent manner in different liver diseases. In this study, we surprisingly found that, rather than displaying cytotoxic or pro-inflammatory features, MAIT cells exhibited a wound healing signature and promoted biliary organoid growth via AREG, which is different from their previously reported functions in liver.[57,62]

Ductular reaction is characterized by maladaptive wound healing response with massive cholangiocyte proliferation and advanced liver fibrosis.[6,9] Cholangiocytes participate in ductular reaction as both initiators and executors,[63] and abnormally proliferated cholangiocytes induce chronic inflammation, causing fibrotic response. Our findings demonstrated that MAIT cells were a key driver of ductular reaction as they displayed wound healing signature and promoted abnormal cholangiocyte proliferation. In addition, AREG is distinct from most other EGF-like growth factors in that it can not only induce a mitogenic signal but can also induce cell differentiation.[28] But we found that MAIT cells activated hepatic stellate cells in the presences of ductular cells, but not hepatic stellate cells alone, suggesting an interaction between reactive ductular cells and myofibroblasts, so-called epithelial-mesenchymal crosstalk. It has been reported biliary epithelial cells can release high levels of IL-8, which acts as a direct profibrotic chemokine in BA.[64] The upregulation of cholangiocyte secretome involves in the epithelial-mesenchymal crosstalk, modulating liver fibrogenesis.[65] Consistently, high abundance of liver MAIT cells were associated with poor survival and liver cirrhosis signature of BA patients. These together demonstrate that, instead of promoting biliary repair, MAIT cells accelerate ductular reaction under an excessive inflammation and fibrosis environment in BA patients, in which cell–cell interactions are involved. Our findings also provide new insights in regulatory mechanisms of MAIT cells in liver diseases.

A recent study found that exogenous IL-33 reversed the suppression of nature ILC2s (nILCs) in RRV infected mouse model.[36] The disruption of the IL-33 signaling promotes a switch of nILC2s to an activated and inflammatory phenotype (iILC2). IL-33 is a potent

Scale bars, 200 μm. Data were analyzed by Student's t test and are presented as mean +SD. *P* value in red, RRV vs. Uninfected; *p* value in black, RRV + Anti-AREG vs. RRV; *p* value in grey, Uninfected + Anti-AREG vs. Uninfected. (**I**) Cell proliferation was analyzed by CCK8 assay. Sorted MAIT cells were co-cultured in the presence or absence of anti-AREG antibody (2 μg/mL). Data were analyzed by Student's t test and are presented as mean ± SD. $^{*}p < 0.05$, $^{**}p < 0.01$, $^{***}p < 0.001$. ns, not significant.

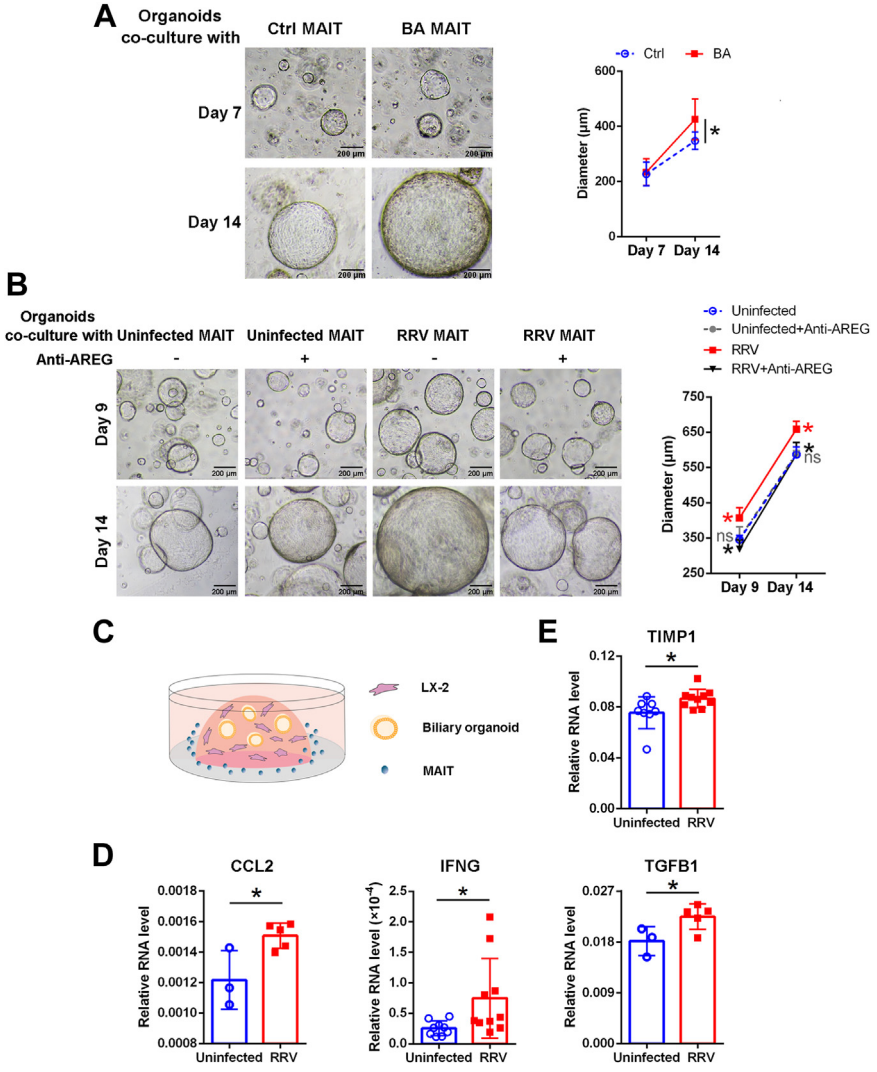

Fig. 6: **MAIT cells promote biliary organoid growth and ductular reaction in BA**. (**A**) Representative images of normal liver biliary organoids and summary data of their average diameters after co-cultured with control (n = 6) or BA (n = 6) MAIT cells for 7 and 14 days. (**B**) Representative images and diameters analysis of biliary organoids co-cultured with uninfected or RRV-primed MAIT cells, in the presence or absence of anti-AREG antibody (2 μg/mL). Data were analyzed by Student's t test and are presented as mean +SD. *p* value in red, RRV vs. Uninfected; *p* value in black, RRV + Anti-AREG vs. RRV; *p* value in grey, Uninfected + Anti-AREG vs. Uninfected. (**C**) Diagram of the biliary organoid - LX-2–MAIT model. Biliary organoids were mixed with LX-2 cells at the ratio of 1:2 in Matrigel, and then co-cultured with uninfected or RRV-primed MAIT cells. (**D and E**) The RNA levels of inflammatory markers (*CCL2*, *IFNG*), profibrogeneic factor (*TGFB1*) and activation marker (*TIMP1*) were analyzed via qPCR in organoid–LX-2, which were co-cultured with uninfected- or RRV-primed MAIT cells for 72 h. GAPDH was used as an internal control. Data were analyzed by Student's t test and are presented as mean ± SD. **p* < 0.05. ns, not significant.

activator of ILC2s and also contributes to M2 differentiation, which can limit acute inflammation. Also, IL-33 can trigger the generation of inducible regulatory T cells.[66] Therefore, exogenous IL-33 stimulation promotes nILC2 stability and AREG expression, decreased inflammation, which together induces epithelial homeostasis and repair in experimental biliary atresia. In this study, however, MAIT cells not only promote cholangiocyte proliferation, but also induced the expression of inflammatory genes *CCL2*, *IFNG* and profibrogeneic factor *TGFB1* (see Fig. 6D), suggesting that MAIT cells accelerate ductular reaction.

It is intriguing that AREG-producing cell types (nILC2s and MAIT cells) perform different functions of promoting biliary repair or ductular reaction. This may due to different liver immune environment. Exogenous IL-33 creates a biliary repairing environment with enhanced level of nILC2s.[36] Without exogenous IL-33, AREG-producing nILC2s were decreased in experimental biliary atresia.[36] In contrast, percentage of

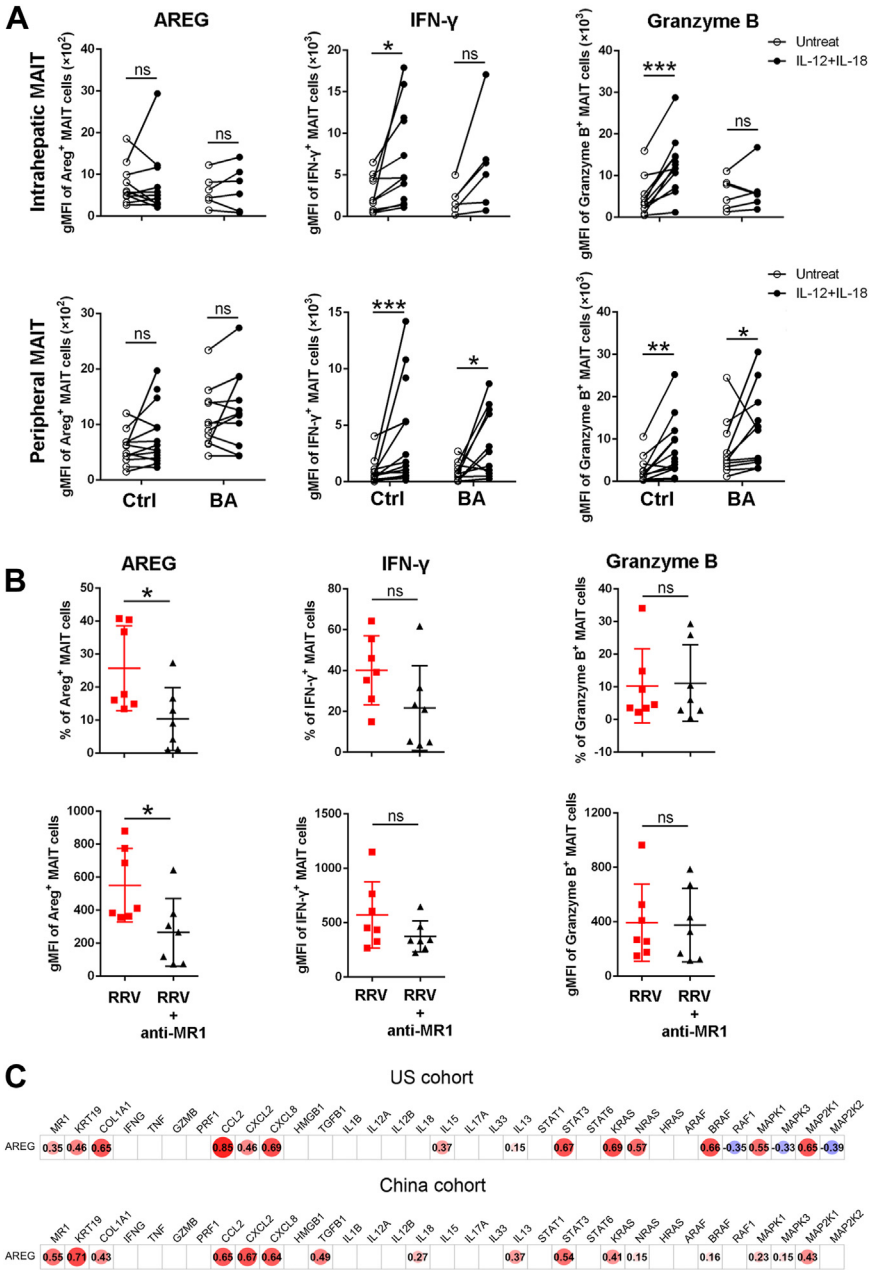

***Fig. 7*: AREG expression is TCR-dependent in MAIT cells and liver AREG expression is correlated with MR1, ductular reaction markers, chemokines and RAS-MAPK in two BA patient cohorts**. (**A**) Intracellular cytokine expression by control (n = 10–17) and BA (n = 6–12) MAIT cells after stimulation with IL-12 + IL-18 for 24 h. Statistical analysis was performed using Student's t test or Mann–Whitney test depending on the distribution turns in to the normal or not. (**B**) Production of cytokines of MAIT cells in a PBMC pool co-cultured with RRV-infected human cholangiocyte H69 in the presence or absence of anti-MR1 blocking antibody (2 μg/mL) was examined at the 18-h time point. Data were analyzed by paired t test. *$p < 0.05$, **$p < 0.01$, ***$p < 0.001$. ns, not significant. (**C**) Correlation matrix between AREG and MR1, ductular reaction markers (*KRT19*, *COL1A1*), chemokines, cytokines and RAS-MAPK in liver gene expression of two BA patient cohorts. Spearman correlation coefficients are shown only in boxes with spearman correlation rho >0.2 and p value < 0.05. Red indicates positive correlation, while blue indicates negative correlation. Dot size is proportional to absolute value of correlation coefficient.

AREG-producting MAIT cells were higher in both human BA livers (see Fig. 3F) and the RRV infected co-culture system (see Fig. 5F) compared to the control. Additionally, AREG was mainly expressed in MAIT cells and increased under RRV infection in the co-culture cell system (see Fig. 5B). Moreover, the same cytokine that promote tissue repair can become dysregulated in the presence of chronic inflammation and an altered cytokine milieu to promote fibrotic responses.[28] For example, AREG played a critical role in the development of TGF-β-induced pulmonary fibrosis.[67] The difference of AREG functions may be related to the upstream and downstream factors, and crosstalk among specific immune cells, cholangiocytes and fibroblasts. In an initial attempt to address this, we found that liver AREG expression was positively correlated with ductular reaction markers (*KRT19* and *COL1A1*), chemokines (CCL2, CXCL2, CXCL8) and RAS-MAPK in two cohorts of BA patients. Future studies will investigate molecular circuit among these factors.

MAIT cells can be activated by two mechanisms, cytokine- or TCR-dependent activation. Inflammatory cytokine signals such as IL-18 and IL-12 drives a signal amplification innate-like response, while combined cytokine and TCR signals trigger a potent antimicrobial response.[17] By contrast, TCR signals alone promote the production of effector molecules associated with tissue repair and homeostasis.[17,23] Our RNAseq analysis revealed that several growth factors were upregulated in liver BA MAIT cells, which were associated with ductular reaction. And flow cytometry showed that liver and peripheral MAIT cells in BA both highly expressed AREG. Our observation that MAIT cells resided around portal tracts in BA livers indicated cholangiocytes or innate immune cells might present MR1 restricted antigen to activate MAIT cells. In line with this observation, blockade of MR1 significantly suppress AREG production. These findings are consistent with the previous studies showing that biliary epithelium activates intrahepatic MAIT cells through MR1[44] and the wound healing program in MAIT cells is stimulated by TCR ligands but not by cytokine-mediated stimulation alone.[24,68]

Of note, age of patients could be a potential confounding factor influencing stage of disease and cell status. In this study, we enrolled control patients (patients with HB, IHC and CC) with age in an appropriate range to minimize the potential confounding effect of age due to difficulty in obtaining perfect age matched control samples as previous studies did[31,38] (Supplemental Table S3). The median age of patients with HB, IHC and CC are 156 days, 72 days and 76 days, respectively. Although patients with HB were older than patients with IHC and CC, we did not observe significant differences in frequency and functions of MAIT cells among these three type of controls, suggesting the confounding effect of age was minimized.

As advanced ductular reaction is predictive of poor survival and promote liver fibrosis, uncovering key mechanisms underlying this processes are essential for future therapeutic design. Our findings provide a potential way for control ductular reaction by diminishing AREG production of MAIT cells via blocking MR1.

Contributors

MHX designed the study, performed the experiments, interpreted the data and wrote the manuscript. SW, PL and DM performed the experiments and interpreted the data. JZ, HC, ZZ, HJ collected clinical samples. JL and HJ curated and analyzed clinical information. HJ and XF revised the manuscript. ZL supervised the project, designed the study, interpreted the data and wrote the manuscript. All authors read and approved the final manuscript.

Data sharing statement

Gene expression data were retrieved from previous deposition in the Gene Expression Omnibus database under accession number GSE15235 for the US cohort and in the Genome Sequence Archive of Beijing Institute of Genomics, Chinese Academy of Sciences under accession number HRA003331 for the China cohort.

RNAseq data of BA MAIT has been deposited in GEO database (GSE217466).

The scRNA-seq data of RRV-primed system has been deposited in GEO database (GSE225177).

Additional data can be obtained from the corresponding author upon reasonable request.

Declaration of interests

The authors declare that they have no competing interests.

Acknowledgements

MR1 5-OP-RU and MR1Ac-6-FP tetramers (Brilliant Violet 421, Human; PE, Mouse) were kindly provided by the NIH Tetramer Core.

Appendix A. Supplementary data

Supplementary data related to this article can be found at https://doi.org/10.1016/j.ebiom.2024.105138.

References

1 Bezerra JA, Wells RG, Mack CL, et al. Biliary atresia: clinical and research challenges for the twenty-first century. *Hepatology*. 2018;68(3):1163–1173.
2 Lendahl U, Lui VCH, Chung PHY, Tam PKH. Biliary Atresia - emerging diagnostic and therapy opportunities. *eBioMedicine*. 2021;74:103689.
3 Sundaram SS, Mack CL, Feldman AG, Sokol RJ. Biliary atresia: indications and timing of liver transplantation and optimization of pretransplant care. *Liver Transpl*. 2017;23(1):96–109.
4 Asai A, Miethke A, Bezerra JA. Pathogenesis of biliary atresia: defining biology to understand clinical phenotypes. *Nat Rev Gastroenterol Hepatol*. 2015;12(6):342–352.
5 Banales JM, Huebert RC, Karlsen T, Strazzabosco M, LaRusso NF, Gores GJ. Cholangiocyte pathobiology. *Nat Rev Gastroenterol Hepatol*. 2019;16(5):269–281.
6 Sato K, Marzioni M, Meng F, Francis H, Glaser S, Alpini G. Ductular reaction in liver diseases: pathological mechanisms and translational significances. *Hepatology*. 2019;69(1):420–430.
7 Zhang Z, Zhong X, Shen H, et al. Biliary NIK promotes ductular reaction and liver injury and fibrosis in mice. *Nat Commun*. 2022;13(1):5111.
8 Richardson MM, Jonsson JR, Powell EE, et al. Progressive fibrosis in nonalcoholic steatohepatitis: association with altered regeneration and a ductular reaction. *Gastroenterology*. 2007;133(1):80–90.
9 Ariño S, Aguilar-Bravo B, Coll M, et al. Ductular reaction-associated neutrophils promote biliary epithelium proliferation in chronic liver disease. *J Hepatol*. 2023;79(4):1025–1036.
10 Glaser SS, Gaudio E, Miller T, Alvaro D, Alpini G. Cholangiocyte proliferation and liver fibrosis. *Expet Rev Mol Med*. 2009;11:e7.

11 Mohanty SK, Lobeck I, Donnelly B, et al. Rotavirus reassortant-induced murine model of liver fibrosis parallels human biliary atresia. *Hepatology*. 2020;71(4):1316–1330.
12 Santos JL, Kieling CO, Meurer L, et al. The extent of biliary proliferation in liver biopsies from patients with biliary atresia at portoenterostomy is associated with the postoperative prognosis. *J Pediatr Surg*. 2009;44(4):695–701.
13 Nomden M, Beljaars L, Verkade HJ, Hulscher JBF, Olinga P. Current concepts of biliary atresia and matrix metalloproteinase-7: a review of literature. *Front Med*. 2020;7:617261.
14 Corbett AJ, Eckle SB, Birkinshaw RW, et al. T-cell activation by transitory neo-antigens derived from distinct microbial pathways. *Nature*. 2014;509(7500):361–365.
15 Eckle SB, Corbett AJ, Keller AN, et al. Recognition of vitamin B precursors and byproducts by mucosal associated invariant T cells. *J Biol Chem*. 2015;290(51):30204–30211.
16 Treiner E, Duban L, Bahram S, et al. Selection of evolutionarily conserved mucosal-associated invariant T cells by MR1. *Nature*. 2003;422(6928):164–169.
17 Provine NM, Klenerman P. MAIT cells in health and disease. *Annu Rev Immunol*. 2020;38:203–228.
18 Magalhaes I, Pingris K, Poitou C, et al. Mucosal-associated invariant T cell alterations in obese and type 2 diabetic patients. *J Clin Invest*. 2015;125(4):1752–1762.
19 Toubal A, Kiaf B, Beaudoin L, et al. Mucosal-associated invariant T cells promote inflammation and intestinal dysbiosis leading to metabolic dysfunction during obesity. *Nat Commun*. 2020;11(1):3755.
20 Bertrand L, Lehuen A. MAIT cells in metabolic diseases. *Mol Metabol*. 2019;27S(Suppl):S114–S121.
21 Hegde P, Weiss E, Paradis V, et al. Mucosal-associated invariant T cells are a profibrogenic immune cell population in the liver. *Nat Commun*. 2018;9(1):2146.
22 Hinks TSC, Marchi E, Jabeen M, et al. Activation and in vivo evolution of the MAIT cell transcriptome in mice and humans reveals tissue repair functionality. *Cell Rep*. 2019;28(12):3249–3262.
23 Leng T, Akther HD, Hackstein CP, et al. TCR and inflammatory signals tune human MAIT cells to exert specific tissue repair and effector functions. *Cell Rep*. 2019;28(12):3077–3091.
24 Lamichhane R, Schneider M, de la Harpe SM, et al. TCR- or cytokine-activated CD8(+) mucosal-associated invariant T cells are rapid polyfunctional effectors that can coordinate immune responses. *Cell Rep*. 2019;28(12):3061–3076.
25 Constantinides MG, Link VM, Tamoutounour S, et al. MAIT cells are imprinted by the microbiota in early life and promote tissue repair. *Science*. 2019;366(6464).
26 du Halgouet A, Darbois A, Alkobtawi M, et al. Role of MR1-driven signals and amphiregulin on the recruitment and repair function of MAIT cells during skin wound healing. *Immunity*. 2023;56(1):78–92.e6.
27 Varelias A, Bunting MD, Ormerod KL, et al. Recipient mucosal-associated invariant T cells control GVHD within the colon. *J Clin Invest*. 2018;128(5):1919–1936.
28 Zaiss DMW, Gause WC, Osborne LC, Artis D. Emerging functions of amphiregulin in orchestrating immunity, inflammation, and tissue repair. *Immunity*. 2015;42(2):216–226.
29 Dong R, Jiang J, Zhang S, et al. Development and validation of novel diagnostic models for biliary atresia in a large cohort of Chinese patients. *eBioMedicine*. 2018;34:223–230.
30 Lam WY, Tang CS, So MT, et al. Identification of a wide spectrum of ciliary gene mutations in nonsyndromic biliary atresia patients implicates ciliary dysfunction as a novel disease mechanism. *eBioMedicine*. 2021;71:103530.
31 Bessho K, Mourya R, Shivakumar P, et al. Gene expression signature for biliary atresia and a role for interleukin-8 in pathogenesis of experimental disease. *Hepatology*. 2014;60(1):211–223.
32 Serinet MO, Wildhaber BE, Broué P, et al. Impact of age at Kasai operation on its results in late childhood and adolescence: a rational basis for biliary atresia screening. *Pediatrics*. 2009;123(5):1280–1286.
33 Luo Z, Shivakumar P, Mourya R, Gutta S, Bezerra JA. Gene expression signatures associated with survival times of pediatric patients with biliary atresia identify potential therapeutic agents. *Gastroenterology*. 2019;157(4):1138–1152.e14.
34 Shneider BL, Magee JC, Karpen SJ, et al. Total serum bilirubin within 3 months of hepatoportoenterostomy predicts short-term outcomes in biliary atresia. *J Pediatr*. 2016;170:211–217.
35 Shneider BL, Abel B, Haber B, et al. Portal hypertension in children and young adults with biliary atresia. *J Pediatr Gastroenterol Nutr*. 2012;55(5):567–573.
36 Russi AE, Shivakumar P, Luo Z, Bezerra JA. Plasticity between type 2 innate lymphoid cell subsets and amphiregulin expression regulates epithelial repair in biliary atresia. *Hepatology*. 2023;78(4):1035–1049.
37 Moyer K, Kaimal V, Pacheco C, et al. Staging of biliary atresia at diagnosis by molecular profiling of the liver. *Genome Med*. 2010;2(5):33.
38 Wang G, Chen H, Sun P, et al. Predictive model containing gene signature and shear wave elastography to predict patient outcomes after Kasai surgery in biliary atresia. *Hepatol Res*. 2023;53(11):1126–1133.
39 Learner J, Goodman NW. Descriptions of correlation. *Lancet*. 1996;348(9021):199–200.
40 Miao YR, Zhang Q, Lei Q, et al. ImmuCellAI: a unique method for comprehensive T-cell subsets abundance prediction and its application in cancer immunotherapy. *Adv Sci*. 2020;7(7):1902880.
41 Yao T, Shooshtari P, Haeryfar SMM. Leveraging public single-cell and bulk transcriptomic datasets to delineate MAIT cell roles and phenotypic characteristics in human malignancies. *Front Immunol*. 2020;11:1691.
42 Broutier L, Andersson-Rolf A, Hindley CJ, et al. Culture and establishment of self-renewing human and mouse adult liver and pancreas 3D organoids and their genetic manipulation. *Nat Protoc*. 2016;11(9):1724–1743.
43 Hukkinen M, Kerola A, Lohi J, et al. Treatment policy and liver histopathology predict biliary atresia outcomes: results after national centralization and protocol biopsies. *J Am Coll Surg*. 2018;226(1):46–57.
44 Jeffery HC, van Wilgenburg B, Kurioka A, et al. Biliary epithelium and liver B cells exposed to bacteria activate intrahepatic MAIT cells through MR1. *J Hepatol*. 2016;64(5):1118–1127.
45 Coots A, Donnelly B, Mohanty SK, McNeal M, Sestak K, Tiao G. Rotavirus infection of human cholangiocytes parallels the murine model of biliary atresia. *J Surg Res*. 2012;177(2):275–281.
46 Mohanty SK, Donnelly B, Temple H, et al. High mobility group box 1 release by cholangiocytes governs biliary atresia pathogenesis and correlates with increases in afflicted infants. *Hepatology*. 2021;74(2):864–878.
47 Wang J, Xu Y, Chen Z, et al. Liver immune profiling reveals pathogenesis and therapeutics for biliary atresia. *Cell*. 2020;183(7):1867–1883.e26.
48 Sharland A, Gorrell MD. Cooperation of innate and adaptive immunity in the pathogenesis of biliary atresia: there's a killer on the run. *Hepatology*. 2009;50(6):2037–2040.
49 Shivakumar P, Campbell KM, Sabla GE, et al. Obstruction of extrahepatic bile ducts by lymphocytes is regulated by IFN-gamma in experimental biliary atresia. *J Clin Invest*. 2004;114(3):322–329.
50 Ortiz-Perez A, Donnelly B, Temple H, Tiao G, Bansal R, Mohanty SK. Innate immunity and pathogenesis of biliary atresia. *Front Immunol*. 2020;11:329.
51 Shivakumar P, Sabla GE, Whitington P, Chougnet CA, Bezerra JA. Neonatal NK cells target the mouse duct epithelium via Nkg2d and drive tissue-specific injury in experimental biliary atresia. *J Clin Invest*. 2009;119(8):2281–2290.
52 Saxena V, Shivakumar P, Sabla G, Mourya R, Chougnet C, Bezerra JA. Dendritic cells regulate natural killer cell activation and epithelial injury in experimental biliary atresia. *Sci Transl Med*. 2011;3(102):102ra94.
53 Soroka CJ, Roberts SJ, Boyer JL, Assis DN. Role of biliary organoids in cholestasis Research and regenerative medicine. *Semin Liver Dis*. 2021;41(2):206–212.
54 Amarachintha SP, Mourya R, Ayabe H, et al. Biliary organoids uncover delayed epithelial development and barrier function in biliary atresia. *Hepatology*. 2022;75(1):89–103.
55 Rahimpour A, Koay HF, Enders A, et al. Identification of phenotypically and functionally heterogeneous mouse mucosal-associated invariant T cells using MR1 tetramers. *J Exp Med*. 2015;212(7):1095–1108.
56 Zhang Y, Kong D, Wang H. Mucosal-Associated Invariant T cell in liver diseases. *Int J Biol Sci*. 2020;16(3):460–470.
57 Böttcher K, Rombouts K, Saffioti F, et al. MAIT cells are chronically activated in patients with autoimmune liver disease and promote profibrogenic hepatic stellate cell activation. *Hepatology*. 2018;68(1):172–186.

58 Yong YK, Saeidi A, Tan HY, et al. Hyper-expression of PD-1 is associated with the levels of exhausted and dysfunctional phenotypes of circulating CD161(++)TCR iVα7.2(+) mucosal-associated invariant T cells in chronic hepatitis B virus infection. *Front Immunol*. 2018;9:472.

59 Bolte FJ, O'Keefe AC, Webb LM, et al. Intra-hepatic depletion of mucosal-associated invariant T cells in hepatitis C virus-induced liver inflammation. *Gastroenterology*. 2017;153(5):1392–1403.e2.

60 Merlini E, Cerrone M, van Wilgenburg B, et al. Association between impaired Vα7.2+CD161++CD8+ (MAIT) and vα7.2+cd161-cd8+ T-cell populations and gut dysbiosis in chronically HIV- and/or HCV-infected patients. *Front Microbiol*. 2019;10:1972.

61 Jiang X, Lian M, Li Y, et al. The immunobiology of mucosal-associated invariant T cell (MAIT) function in primary biliary cholangitis: regulation by cholic acid-induced Interleukin-7. *J Autoimmun*. 2018;90:64–75.

62 van Wilgenburg B, Scherwitzl I, Hutchinson EC, et al. MAIT cells are activated during human viral infections. *Nat Commun*. 2016;7:11653.

63 Gouw AS, Clouston AD, Theise ND. Ductular reactions in human liver: diversity at the interface. *Hepatology*. 2011;54(5):1853–1863.

64 Dong R, Zheng S. Interleukin-8: a critical chemokine in biliary atresia. *J Gastroenterol Hepatol*. 2015;30(6):970–976.

65 Cai X, Tacke F, Guillot A, Liu H. Cholangiokines: undervalued modulators in the hepatic microenvironment. *Front Immunol*. 2023;14:1192840.

66 Schiering C, Krausgruber T, Chomka A, et al. The alarmin IL-33 promotes regulatory T-cell function in the intestine. *Nature*. 2014;513(7519):564–568.

67 Schramm F, Schaefer L, Wygrecka M. EGFR signaling in lung fibrosis. *Cells*. 2022;11(6):986.

68 Hinks TSC, Zhang XW. MAIT cell activation and functions. *Front Immunol*. 2020;11:1014.